Journal of Mammalogy, XX(X):1–16, 2020
DOI:10.1093/jmammal/gyaa107

The relationship between molar morphology and ecology within *Neotoma*

Catalina P. Tomé,*, Winifred Whiteman-Jennings, and Felisa A. Smith

School of Biological Sciences, University of Nebraska–Lincoln, 4 Manter, Lincoln, NE 68506, USA (CPT)
Department of Biology, University of New Mexico, Albuquerque, NM 87131, USA (CPT, WW-J, FAS)
Department of Math, Science and Engineering, Central New Mexico Community College, Albuquerque, NM 87106, USA (WW-J)

** Correspondent: ctome2@unl.edu*

The extensive diversity in dental form across mammals and its strong relationship with function provides insights into the diet, habitat, and behavior, of both extant and extinct taxa. Understanding the extent of variation in dental morphology across species allows for more accurate identification of fossils and a better ability to infer relationships between form and function and ecology. We examined variation in the size and shape of the first upper molar among the genus *Neotoma*. We employed elliptical Fourier analysis to quantify differences in the shape of 2D outlines for 23 populations and six species of *Neotoma*, varying in body size and habitat preference. As expected, molar length is a strong predictor of body size and is significantly and negatively correlated with temperature, particularly in species whose ranges span large latitudinal gradients. We found that differences in molar shape separate species into three general morpho-groups, with no evidence of a phylogenetic signal. While outline analysis could not robustly classify all molars to the species level, it did perform well for *Neotoma cinerea*, probably because of the greater degree of folding and more acute angling of molar lophs. In contrast, wider lophs with shallower enamel infolding was characteristic of species specializing on softer, more succulent resources (i.e., *Neotoma albigula* and *Neotoma micropus*). *Neotoma floridana* were inaccurately classified to species in the majority of cases, but were the only molars correctly identified to locality 100% of the time, suggesting that dietary specializations at a local level may drive morphological changes within the species as well as across the genus.

Key words: cricetid tooth form, geometric morphometrics, inter-/intraspecific dental morphology

La gran diversidad que existe en la morfología de molares en los mamíferos y su fuerte relación con su función provee información sobre la dieta, medio ambiente y comportamiento de especies existentes y extintas. Comprender la variación en la morfología dental de especies ayuda a identificar fósiles y a inferir las relaciones entre la forma y su función y la ecología. En este estudio examinamos la variación en tamaño y forma del primer molar superior del género *Neotoma*. Aplicamos análisis elípticos de Fourier para cuantificar las diferencias en la forma entre contornos 2D para 23 poblaciones y 6 especies de *Neotoma*, con variaciones en el tamaño del cuerpo y la preferencia de hábitat. Como era esperado, el largo del molar predice el tamaño del cuerpo y está negativamente correlacionado con la temperatura del medio ambiente, especialmente para especies cuyos rangos de distribución abarcan grandes gradientes latitudinales. Encontramos que las diferencias en la morfología del molar permiten identificar 3 grupos morfológicos generales, sin evidencia de una correlación filogenética. El análisis de contorno no permitió clasificar los molares al nivel de especies, pero demostró ser apropiado para clasificar *Neotoma cinerea*, probablemente por el grado del plegado y por los ángulos más prominentes en los contornos de los lóbulos molares. En contraste, los molares con ángulos más anchos y pliegues de esmalte menos prominentes son más característicos de especies con dietas basadas en recursos más suaves y suculentos (e.g., *Neotoma albigula* y *Neotoma micropus*). *Neotoma floridana* no se pudo clasificar al nivel de especie en la mayoría de los casos, pero sus molares fueron correctamente asociados en un 100% a la región geográfica

en todos los casos, lo cual sugiere que especialización de dieta al nivel de población puede afectar cambios morfológicos dentro de especies y del género.

Palabras Clave: cricétidos, forma de los dientes, morfología dental inter/intra específica, morfometría geométrica

Mammals demonstrate an incredible diversity in dental form and function that mirrors a broad range of ecological niches and diets. The evolution of teeth in mammals has been widely studied, with characteristics of tooth size, shape, and masticatory mechanisms of the jaw, correlating with diet (Janis and Fortelius 1988; Ungar and Williamson 2000; Schmidt-Kittler 2002; Evans and Sanson 2003; Samuels 2009; Ungar 2010). The cheek teeth of herbivores, for example, are generally high-crowned with increased enamel folding. This allows for a greater grinding capacity at the occlusal surface to help deal with a broad spectrum of resources and high quantities of abrasive and tough plant matter or grit intake and increased wear rates generally associated with open, grassland habitats (Janis and Fortelius 1988; Janis 1995; Williams and Kay 2001; Jardine et al. 2012; Samuels and Hopkins 2017). The morphology of carnivoran teeth, on the other hand, is better suited for slicing, with a higher degree of shearing surfaces, either due to size or crests, associated with groups consuming higher proportions of vertebrates compared to invertebrates or fruits (Van Valkenburgh 1989; Strait 1993a, 1993b; Meiri et al. 2005). Enamel is durable and thus teeth are well preserved in the fossil record (Van Valkenburgh 1994). Consequently, variation in dental morphology provides a means of identification for both fossil and modern mammal taxa (Carrasco 2000; Hillson 2005; Ungar 2010), as well as insights into their ecology (Van Valkenburgh 1994; Thomason 1997). While the use of dental form to study adaptations and diet is extremely useful, it is important to account for factors that may constrain the precision of identifications and inferences (Gailer et al. 2016).

The evolution and life history of a mammal influences the morphological variation in dental form. Genetic and developmental constraints may limit the adaptation of form to dietary function (Evans and Sanson 2003; Evans et al. 2007; Ledevin et al. 2010; Rodriguez et al. 2013). Tooth characteristics of an individual also can be altered throughout their lifetime. Wear can play an important role in changing the shape of the occlusal surface, sometimes in an uneven manner (Harris 1984; Guérécheau et al. 2010; Ledevin et al. 2010). For example, a study of bank voles found that wear (age) was the primary source of variation across the occlusal surface of the third upper molar, while intraspecific variation was tied to the presence or absence of an additional posterior structure due to developmental constraints on size of the molar (Ledevin et al. 2010). Characterizing dental variation within a genus thus improves accuracy of identification of materials and the interpretation of the relationships between tooth form and ecology across space and time.

Here we focus on the genus *Neotoma.* We first investigate whether the first upper molar accurately distinguishes between species varying in size and ecology. Second, we investigate the relationship between tooth morphology and habitat that may arise because of differences in climate and vegetation. Woodrats are widespread across most of North America (Fig. 1), extending from the Northwestern Territories of Canada to Nicaragua in Central America and from the west to east coast of North America (Hall 1981; Betancourt et al. 1990). The genus includes adult animals weighing between 80 and > 500 g, who occupy a diverse array of habitats, from mountainous pine forests to desertic shrublands, and subsist on a wide variety of vegetative resources, including foliage, berries, cacti, and nuts (Wiley 1980; Cornely and Baker 1986; Macêdo and Mares 1988; Jones and Hildreth 1989; Carraway and Verts 1991; Smith 1997; Verts and Carraway 2002). Moreover, *Neotoma* have played an important role in late Pleistocene paleoecological studies because of the detailed plant and animal records preserved within their paleomiddens (e.g., Betancourt et al. 1990; Smith et al. 1995, 2009; Smith and Betancourt 2003, 2006). However, *Neotoma* skeletal remains are difficult to identify to species, with identifications generally relying on isolated molars (Harris 1984).

We use geometric morphometrics to quantify the morphological variation across several species of the genus *Neotoma*, using an elliptical Fourier analysis of the first upper molar. Geometric morphometrics permits quantification of variation across similar morphological features by considering the form or shape of an object independently of size or orientation (Claude 2008; Zelditch et al. 2012). Physical features are recorded using different shape coordinate systems (commonly landmarks or outlines) to compare deviations of morphological features across specimens. Landmarks placed on homologous anatomical points are used to assess disparity across similar structures. In contrast, 2D outlines capture the perimeter of a shape and take into account curves along the outer profile of each specimen; this can then be used to determine similarities and differences in shape across specimens (Bookstein 1997; Adams 1999; Adams et al. 2004). Previous studies using outline analysis have employed elliptical Fourier analysis, in which closed outlines (made up of x, y coordinates) are transformed into a set of harmonic ellipses with four coefficients each. The elliptical Fourier analysis is used to produce a matrix of coefficients that describe each shape in the data set, which then can be used in multivariate analyses (Kuhl and Giardina 1982; Bonhomme et al. 2014). Applications of outline analysis include considering morphological variation in mammal molars (Renaud et al. 1996; Gómez Cano et al. 2013; Mitchelle 2016), rodent mandibles (Renaud and Millen 2001), human cranial deformation (Frieß and Baylac 2003), leaf shape (Adebowale et al. 2012), and pollen grains (Bonhomme et al. 2013), among others.

Neotoma have high-crowned, rooted molars, with three confluent or offset lophs (Zakrzewski 1993; Figs. 2A–F). However, there are differences within the clade: *Neotoma cinerea* and

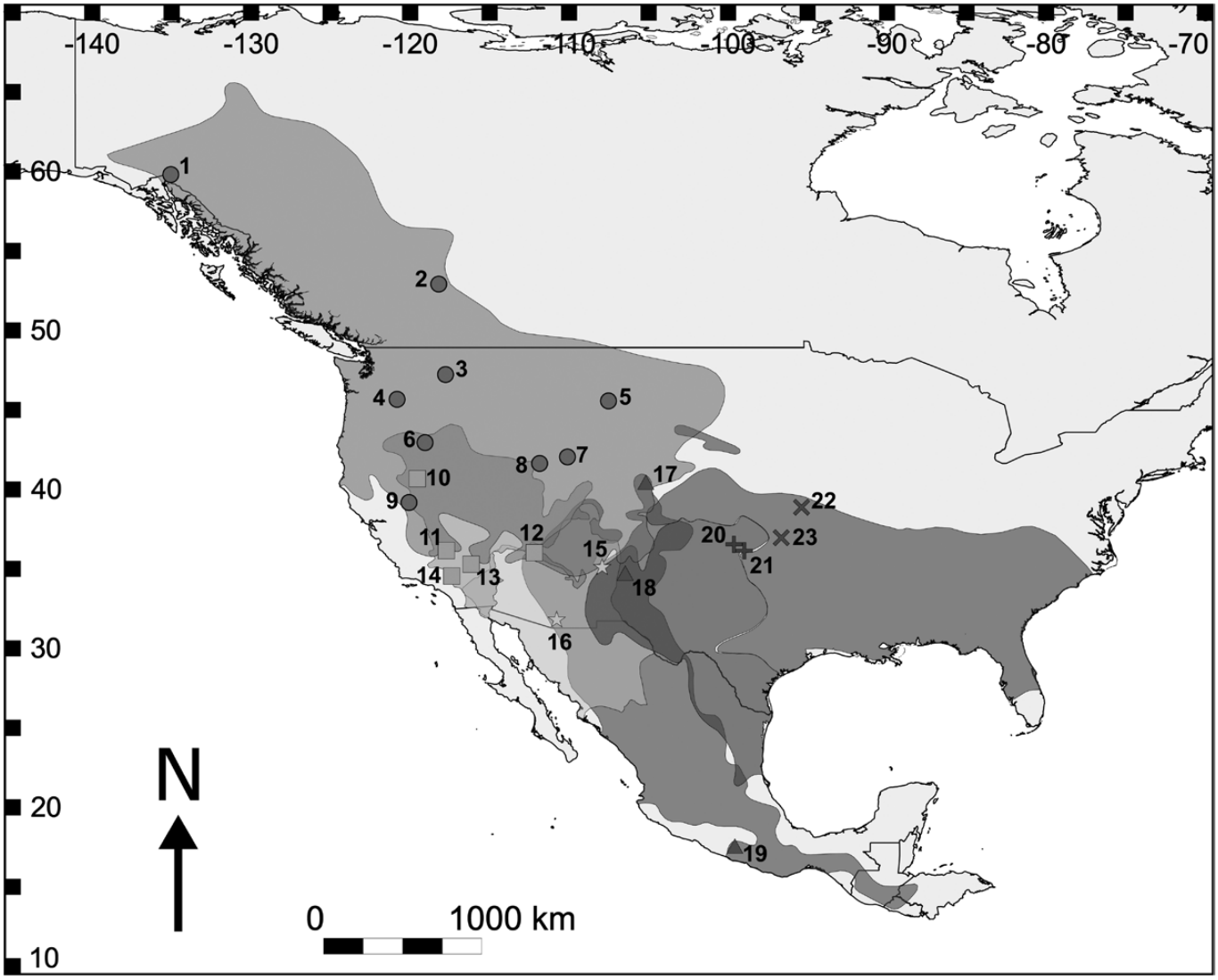

Fig. 1.—*Neotoma* species distributions across North America. Distributions and localities of *Neotoma* used in study shown for species: *Neotoma albigula* (star), *Neotoma cinerea* (circle), *Neotoma floridana* (x cross), *Neotoma lepida* (square), *Neotoma mexicana* (triangle), and *Neotoma micropus* (+ cross). Localities are numbered as follow: 1) Bennett City, 2) Jasper House, 3) Spokane, 4) Klickitat, 5) Big Horn, 6) Harney, 7) Sweetwater, 8) Bear Lake, 9) Donner, 10) Secret Valley, 11) Coso, 12) Lees Ferry, 13) Panamint Valley, 14) Oro Grande, 15) Grants, 16) Pima, 17) Loveland, 18) Manzano Mountains, 19) Omiltemi, 20) Fort Supply, 21) Major, 22) Wakarusa, and 23) Osage. Latitude and longitude given along top and left of figure. Map was produced in QGIS Desktop 3.03, using species distributions from IUCN (2018).

Neotoma mexicana generally exhibit thinner lophs and deeper fold patterns between the lophs, while *Neotoma albigula* and *Neotoma lepida* tend to have more rounded lophs with shallower enamel folding patterns. While woodrat molars are straightforward to identify to genus, it is more difficult to identify species within the group (Repenning 2004). First molars are the most informative when trying to distinguish among species of *Neotoma*. A previous study examining the first lower molar (m1) within the genus, for example, proposed that the presence of a lateral dentine tract could be used to differentiate *N. cinerea*, *N. goldmani*, *N. lepida*, *N. mexicana*, and *N. stephensi* from *N. albigula*, *N. floridana*, and *Neotoma micropus* (Harris 1984).

The first upper molar (M1) of *Neotoma* is of particular interest because of variation in an anterolingual fold on the anteroloph across the different species (Fig. 2). Past studies have found that the anterolingual fold generally is shallow or lacking in *N. stephensi* and *N. lepida*, more developed in *N. cinerea*, *N. mexicana*, and *N. micropus*, and is considered highly variable in *N. floridana* (Zakrzewski 1993; Repenning 2004). Variation in the fold has been reported in coastal and desert populations of *N. lepida* in California and Mexico (Patton et al. 2007). Thus, this feature may provide an additional metric for identification. Studies have had varying levels of success separating fossil *Neotoma* using characteristics such as toothrow width, breadth of the second loph of the first molar, the rootward extent of the anteromedial groove, and the presence or absence of pits at the base of enamel reentrants, among other traits (Dalquest et al. 1969; Zakrzewski 1993; Repenning 2004). However, earlier work has not included consideration of the substantial variation within each species. Moreover,

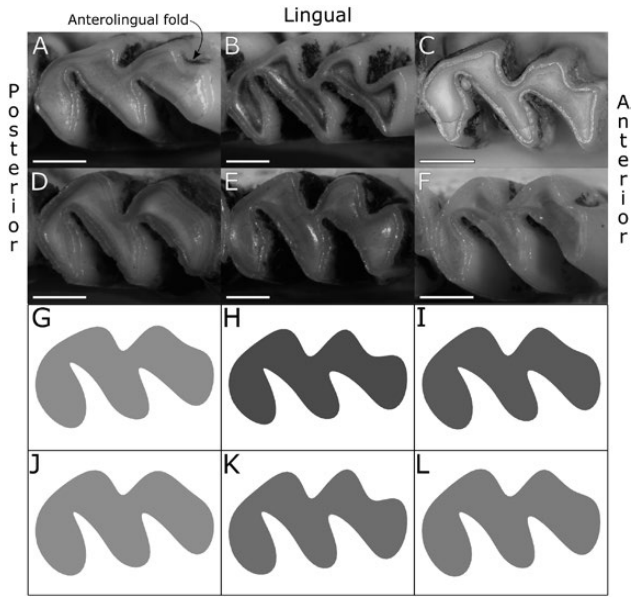

Fig. 2.—Photographs and mean shape of *Neotoma* molar. Photographs of the first upper left molars of six species of *Neotoma*: (A) *Neotoma albigula*, (B) *Neotoma cinerea*, (C) *Neotoma floridana*, (D) *Neotoma lepida*, (E) *Neotoma mexicana*, and (F) *Neotoma micropus*. Scale bar displays 1 mm of length. Mean shape of the first upper molar of (G) *N. albigula*, (H) *N. cinerea*, (I) *N. floridana*, (J) *N. lepida*, (K) *N. mexicana*, and (L) *N. micropus* produced from elliptical Fourier coefficients.

geographic variation in morphology between and within species may be related to environmental variables (Travis 1994), or potentially to diet. The six *Neotoma* species selected for our study have varying degrees of overlap in both geographic distribution and resource use.

The white-throated woodrat (*N. albigula*) is found primarily in arid regions across the southwestern United States and into central Mexico (Fig. 1; Hall 1981; Macêdo and Mares 1988). *Neotoma albigula* typically is associated with cactus; in the Sonoran Desert up to 40–45% of the diet is *Opuntia*, which serves as both a food and water source (Vorhies and Taylor 1940; Olsen 1976; Orr et al. 2015). In the absence of *Opuntia* and *Yucca*, populations in Colorado and across the Great Basin also consume large quantities (as high as 35% of their diet) of *Juniperus* sp. (Finley 1958; Dial 1988).

The bushy-tailed woodrat (*N. cinerea*) has the widest geographic range in the genus, ranging from the Yukon and Northwest Territory of Canada to the southwestern United States, and from the Pacific coast to the Great Plains (Fig. 1; Hall 1981; Smith 1997). The range covers > 30 degrees of latitude and a wide variety of habitats and climatic conditions. *Neotoma cinerea* are predominantly rock-dwellers, but can be found across vastly different habitats, such as desertic piñon–juniper woodlands, coastal deciduous–coniferous forests, and mountainous pine, Douglas-fir, and aspen forests, as long as rock shelter is available (Finley 1958; Brown 1968; Hickling 1987; Smith 1997). The bushy-tailed woodrat has a generalized diet of leafy vegetation, with preferences varying among subspecies and populations (Finley 1958; Smith 1997). Populations in Colorado, for example, specialize on aspen, Douglas-fir, juniper, prickly-pear, and hackberry (Finley 1958). Coastal *N. cinerea* eat higher quantities of Douglas-fir, spruce, and hemlock, along with a variety of other vegetation and berries (Carey 1991).

The eastern woodrat (*Neotoma floridana*) occupies both arid and subtropical areas, ranging across the eastern United States from the Atlantic coast (from Florida to North Carolina) to the Great Plains (northern Colorado to southern Texas; Fig. 1; Wiley 1980; Hall 1981). It is associated predominantly with deciduous forests, although in Colorado, cactus, as well as skunkbush, greasewood, and *Yucca* have been reported in the diet (Rainey 1956; Finley 1958). *Neotoma floridana* often specializes on acorns, osage orange, and oak berries across its range along with other green vegetation, fruits, and seeds (Murphy 1952; Rainey 1956; Finley 1958; Wiley 1980).

The desert woodrat (*N. lepida*) is found in arid habitats in the western United States from southern Oregon and Idaho through the Baja California peninsula of Mexico (Fig. 1; Hall 1981; Verts and Carraway 2002). *Neotoma lepida* make use of various xeric-adapted plants and tends to specialize on a few resources at a population level. Different populations in California have been shown to focus on creosote, sage, oak, juniper, and *Yucca*, while consuming more juniper in Utah, shadscale and prickly-pear in Idaho and Colorado (Finley 1958; Cameron and Rainey 1972; Meserve 1974; Verts and Carraway 2002).

The Mexican woodrat (*N. mexicana*) ranges across 20 degrees of latitude, from the southwestern United States (northern Colorado) to western Honduras (Fig. 1; Hall 1981; Cornely and Baker 1986). *Neotoma mexicana* is considered to have a relatively generalized diet, typically consuming foliage over other plant parts, and eating relatively little cactus or grass (Finley 1958). Taking advantage of abundant resources, *N. mexicana* eats a variety of plants, generally shrubs and forbs. The Mexican woodrat makes greater use of conifer needles, scrub oak, and juniper in Colorado where it is found most commonly among oak and piñon–juniper, and consumes acorns and juniper berries in New Mexico and Texas, among other green vegetation, seeds, and nuts (Finley 1958; Cornley and Baker 1986; Schmidly and Bradley 2016).

The southern plains woodrat (*N. micropus*) generally is found in semiarid regions in the southern Great Plains of the United States and northeastern Mexico (Fig. 1; Hall 1981; Braun and Mares 1989). *Neotoma micropus* uses cactus across its range. *Opuntia* is a primary food source for *N. micropus* in both Colorado (as tree cactus) and Texas (as prickly-pear—Finley 1958; Schmidly and Bradley 2016). An absence of tree cactus leads to a greater use of prickly-pear and *Yucca* (Finley 1958). Across the species' range, *N. micropus* eats mixed quantities of other green vegetation, fruits, and seeds (Finley 1958; Braun and Mares 1989).

Based on earlier studies, we suspect there may be a phylogenetic influence on dentition within the genus, although convergent morphologies also could arise if animals occupy

similar environments or consume similar resources. We predict that species that overlap in their use of similar foods, such as a high use of cacti in the more desertic-adapted *N. albigula* and *N. lepida*, will share comparable characteristics in molar shape driven by the processing of certain resources and occupancy of similar environments.

Materials and Methods

We examined 230 *Neotoma* specimens from six species widespread across the western United States: *N. albigula* ($N = 20$), *N. cinerea* ($N = 90$), *N. floridana* ($N = 20$), *N. lepida* ($N = 50$), *N. mexicana* ($N = 30$), and *N. micropus* ($N = 20$) and 23 localities (Appendix I; Fig. 1). Specimens were from the Smithsonian National Museum of Natural History (USNM) in Washington, D.C., and the James F. Bell Museum of Natural History (MMNH) at the University of Minnesota (St. Paul, Minnesota; Appendix I).

Specimen selection and preparation.—We examined variation within species by localities within the geographic distribution that encompassed the range of climatic conditions and dietary preferences, although this was restricted by low sample size among *N. albigula*, *N. floridana*, and *N. micropus*. Most specimens within a site were collected within roughly the same time frame (e.g., 3–5 years), with the exceptions of Bear Lake, Harney, and Omilteme, where specimens represented much longer time frames (e.g., 50, 20, and 60 years, respectively). Because we were interested in population-level variation as well, a site had to have 10 or more adult individuals to be included.

Neotoma teeth were assigned a wear index from 1 to 5 using the following criteria: 1) little to no wear present, with enamel of the first molar not worn flat; 2) enamel of first molar flat but little wear present; 3) molar worn but no rounding of enamel border is present; 4) molar worn with slight rounding of enamel borders; 5) molar heavily worn and rounding of enamel edges obscures outlines. Because tooth wear can cause changes to the occlusal surface in *Neotoma* (Repenning 2004), molars with wear indices either of 1 (representing juveniles) or 5 (very old individuals whose excess wear led to poorly articulated teeth) were not used in producing outlines of molars. Thus, our samples all reflect animals with wear indices 2–4. A separate set of analyses were run to test for potential biases introduced due to our wear indices (Supplementary Data SD1, SD2, SD3).

The occlusal surface of the upper first molar (M1) was photographed using either an Olympus Microscope DP12 (Olympus Corporation, Tokyo, Japan), or a Canon EOS 70D with a Canon EF 50mm f/1.8 STM lens (Canon Inc., Tokyo, Japan). Photographs were digitized into two-dimensional outlines of the left M1. Right UM1s were used for specimens whose left molar was missing or broken, with images being flipped horizontally to mirror the orientation of a left molar. Outlines followed the outer edge of enamel at the crown of the molar and were saved as x, y coordinates using the polygon tool in ImageJ 1.50i (Rasband 1997–2018). Outlines had an average of 178 points (± 56 coordinates). Molar area was measured using the polygon tool and length was measured using the straight-line tool in ImageJ 1.50i. Each specimen was measured twice to minimize measurement error; all length measurements had a standard error below 0.05. The final data set consisted of 230 molars. All analyses were carried out using R 3.3.3 (R Development Core Team 2016) within RStudio 1.0.136 (RStudio Team 2016).

Environmental variables.—To examine interactions between climate, vegetation, and molar morphology, we obtained locality specific variables from the Climate of Western North America data set (ClimateWNA), the Parameter-Elevation Regressions on Independent Slopes Model data set (PRISM), and the Moderate Resolution Imaging Spectroradiometer (MODIS) data set from NASA's Earth Observing System Data and Information System (EOSDIS) database. ClimateWNA provides scale-free historical (1901–2014) climate data throughout North America by locally downscaling historical PRISM and Australian National University Spline (ANUSPLIN) data (Wang et al. 2016). Most of the climate data were extracted from ClimateWNA ($N = 146$). Because ClimateWNA only extends back to 1901, climate data for specimens collected between 1895 and 1900 ($N = 39$) were downloaded from PRISM (Daly et al. 1994, 2008). PRISM models historical data using 30-year normals from North American station data for localities across the United States.

For each site and year of collection, we extracted mean annual temperature (MAT), maximum annual temperature (MxAT), minimum annual temperature (MnAT), and mean annual precipitation (MAP) using locality longitude, latitude, and elevation. Specimens collected prior to 1895 or those without exact locality information were excluded ($N = 45$), including all specimens from Jasper House (*N. cinerea*), Coso (*N. lepida*), and Panamint Valley (*N. lepida*). Climate analyses were undertaken on the remaining 185 specimens.

Because most specimens were collected between 1880 and 1970, precise vegetation indices were not available for most years. Therefore, in order to include an index for potential differences in vegetation presence across our localities, we used the Normalized Difference Vegetation Index (NDVI) of the MODIS data from NASA's Earth Observing System Data and Information System (EOSDIS; https://earthdata.nasa.gov/about). This data set provided consistent NDVIs across North America, with adequate spatial resolution for comparisons among our localities. We used the MODIS/Terra Vegetation Indices Monthly L3 Global 0.05 Deg CMG V006 (MOD13C2.006) data set, which has a 0.5° spatial and monthly temporal resolution of NDVI from February of 2000 to the present (Didan et al. 2015). NDVI is a calculated ratio using near-infrared radiation (NIR) to red reflectance (Red): $NDVI = (NIR - Red)/(NIR + Red)$. This normalized transform gives values between 0 and 1, with 1 indicating the largest proportion of green leaves present and 0 indicating the absence of vegetation (Didan et al. 2015). We used latitude and longitude to extract locality NDVIs from the MOD13C2.006 February 2000 raster file data using QGIS Desktop 3.03.

Data analysis.—We examined variation in molar size (length and area) within and across species localities of *Neotoma*

using analysis of variance (ANOVA) and Tukey's Honestly Significant Difference tests for multiple comparisons of the means. Kruskal–Wallis and Wilcoxon rank sum tests were used for localities where assumptions for parametric analyses were not met (e.g., *N. lepida* and *N. mexicana*). We used multiple linear regressions with Akaike's information criterion (AIC) to investigate whether molar size correlated with climate (MAP, MAT, MxAT, or MnAT) or vegetation (NDVI). Furthermore, because cheek teeth have been shown to sometimes scale isometrically with body size within certain taxa (Fortelius 1985), we used linear regressions to evaluate the relationship of molar length and area with body size using body length estimates (total length minus tail length) for each specimen.

Outlines (*x*, *y* coordinates) were imported into R and a general Procrustes superimposition (GPA) was carried out prior to running an elliptical Fourier analysis (EFA). The GPA was undertaken to account for any differences in the size, orientation, and location of outlines, which can affect the EFA (Rohlf 1990). Because outlines were defined by a different number of points on each specimen, 10 configuration landmarks were placed following the same order (starting at landmark 1) at regular positions given by consistent features along the molar outlines for use in reorientation. The GPA aligns and scales outlines to minimize differences between each outline and the mean configuration. The configuration landmarks were used to calculate rotation parameters for each outline (Rohlf and Slice 1990; Frieß and Baylac 2003; Claude 2008; Zelditch et al. 2012). An elliptical Fourier analysis was then carried out on the outlines. EFA was used to convert (*x*, *y*) coordinates for each closed outline into a harmonic ellipse. Each harmonic ellipse was described by four coefficients (two for each *x* and *y* coordinate) which defined the shape of the original outline (Kuhl and Giardina 1982; Bonhomme et al. 2014). Here, we chose to use 10 harmonics, accounting for 99% of the total harmonic power, such that the shape of each molar was approximated using 40 elliptical Fourier (EF) coefficients.

Principal components analysis (PCA) was carried out on the EF coefficients covariance matrix to characterize variation in the shape of M1 across *Neotoma.* PCA reduced the number of EF coefficients into independent eigenvectors (PCs) that describe the primary sources of variation in molar shape (Table 1).

Table 1.—Results of principal components analysis based on elliptical Fourier coefficients covariance matrix. Eigenvalues, proportional, and cumulative contribution for the first nine (of 40) principal components, explaining a total of 94% variation in molar outline shape across *Neotoma* species. Principal components 10–40 each contained less than 1% of variance in the data.

Principal component	Eigenvalues	Proportion (%)
1	0.513	51.3
2	0.150	15.0
3	0.100	10.0
4	0.058	5.8
5	0.046	4.5
6	0.025	2.5
7	0.020	2.0
8	0.017	1.7
9	0.011	1.1

We plotted the PCs against each other to visualize M1 shape relationships across *Neotoma* species. An inverse Fourier transform was used to visualize the effect of each PC on the shape of the molar outline on the PC scatterplots.

A jackknife validation within a canonical variate analysis (CVA) was used to test for differences in molar outlines of species across the genus and across localities at the species level. CVA uses linear combinations of variables to maximize discrimination among groups, and uses the within-group variation to scale the canonical variates (Zelditch et al. 2012). A CVA was undertaken on the scores of the first three PCs (below which each PC accounted for less than 10% of variation in molar shape) to test whether specimen molars could be reliably assigned to species.

We computed multiple linear regressions with AIC using a stepwise algorithm with both forward and backward selection on size measurements and scores for the first three PCs. Here we examined whether shape of the upper first molar was associated with regional climate or vegetation. Outline analyses were carried out using the R packages Momocs 1.3.0 (Bonhomme et al. 2012) and Morpho 2.6 (Schlager 2017).

Phylogenetic analysis.—We examined the potential effect of phylogeny on molar shape following Matocq et al. (2007). To reproduce the general *Neotoma* tree topology from Matocq et al. (2007), we downloaded all sequenced loci (four mitochondrial: *12S*, *16S*, *COII*, *cytb*; four nuclear: *MLR*, *MYH6*, *EN2*, *FGB*) for a representative from each species (*N. albigula*, NK50148; *N. cinerea*, BYU17790; *N. floridana*, TK52109; *N. lepida*, MVZ197379; *N. mexicana*, TK78350; *N. micropus*, TK54559) from GenBank. Sequences were aligned using MUSCLE v3.8 (Edgar 2004). We generated a maximum-likelihood phylogeny in RaxML v. 8.2 (Stamatakis 2014) with 10,000 iterations and a 25% burn-in under a general time reversible (GTR) model of evolution. The resulting Newick tree was imported into R and analyzed using Geomorph 3.0.6 (Adams et al. 2018). We tested for phylogenetic signal ("physignal," 10,000 iterations) against morphology data comprised of 120 mean molar shape coordinates per species. The function "plotGMPhyloMorphoSpace" was used to produce the plot of the phylogeny across principal dimension of tangent space based on the Procrustes-aligned 230 elliptical coordinates.

Results

Size of the first upper molar was significantly different in both length (ANOVA: $F_{5,224} = 77.22$, $P < 0.001$) and area (ANOVA: $F_{5,224} = 8.33$, $P < 0.001$) across *Neotoma* species (Table 2; Fig. 3). Furthermore, both the area and length of M1 were significantly correlated with each other (linear model: $F_{1,228} = 186$, adjusted $R^2 = 0.45$, $P < 0.001$) and total body length. However, molar length acted as a better proxy for body size (linear model: $F_{1,197} = 274.9$, adjusted $R^2 = 0.58$, $P < 0.001$) than molar area ($F_{1,197} = 119.4$, adjusted $R^2 = 0.37$, $P < 0.001$). These results were not surprising given that there are significant differences in body size among *Neotoma* species. For example, *N. cinerea* and *N. lepida* had molar lengths that differed significantly from all other

Table 2.—Results of the Tukey multiple comparisons of the means tests for ANOVAs run on the molar area and molar length across *Neotoma* species and localities. Kruskal–Wallis and Wilcoxon rank sum tests are reported for molar area of *Neotoma lepida* and *Neotoma mexicana.* Significant differences are denoted as follows: *$P < 0.05$, **$P < 0.01$, and ***$P < 0.001$. Only species or localities with significant differences shown.

	M1 length	M1 area
Across species		
N. albigula–N. cinerea	***	
N. albigula–N. floridana		
N. albigula–N. lepida	***	
N. albigula–N. mexicana		
N. albigula–N. micropus	*	
N. cinerea–N. floridana	***	
N. cinerea–N. lepida	***	***
N. cinerea–N. mexicana	***	
N. cinerea–N. micropus	**	
N. floridana–N. lepida	***	
N. floridana–N. mexicana		
N. floridana–N. micropus		
N. lepida–N. mexicana	***	
N. lepida–N. micropus	***	***
N. mexicana–N. micropus		

	M1 length	M1 area
Across localities		
N. cinerea		
Bear Lake–Jasper House	***	
Big Horn–Sweetwater	*	
Donner–Jasper House	***	
Harney–Jasper House	*	
Jasper House–Spokane	**	
Jasper House–Sweetwater	***	
Klickitat–Sweetwater	*	
N. floridana		
Osage–Wakarusa		*
N. lepida		
Coso–Oro Grande	**	***
Coso–Panamint Valley		*
Coso–Secret Valley		*
Lees Ferry–Oro Grande		*
Oro Grande–Panamint Valley		***
Oro Grande–Secret Valley	*	
Panamint Valley–Oro Grande		**
N. mexicana		
Loveland–Manzano Mountains		**
Loveland–Omiltemi	**	***
Manzano Mountains–Omiltemi	**	

species and each other, while *N. floridana*, *N. Mexicana*, and *N. micropus* were indistinguishable (Table 2; Fig. 3). Differences in molar area were found only between *N. lepida* and *N. cinerea* and *N. micropus* (Table 2). The majority of these relationships are maintained independent of molar wear (Supplementary Data SD4). With the exception of *N. albigula* and *N. micropus*, M1 length and area (and thus body size) also were found to be significantly different across various populations within the same species (Table 2).

Molar shape.—Principal components analysis of the EF coefficients found the first nine PCs to account for about 94% of the variance in molar shape (Table 1), with size removed by the GPA. The EFA found three general "morpho"-groups across *Neotoma*. Two separate groups contain most of the variation in molar shape. These are *N. cinerea* and *N. mexicana* in one group, and *N. albigula* and *N. lepida* in the other. However, *N. floridana* and *N. micropus* are less differentiable from these and from each other. Fifty percent confidence ellipses for species molar morphology show a large degree of overlap across *N. floridana* and *N. micropus* with the four remaining species across PC1–3 (Figs. 4A and 4B). Comparisons of the first three PCs (Figs. 4A and 4B), which account for 76.3% of molar shape variation, separate species into three general morpho-groups: Group A (*N. cinerea* and *N. mexicana*), Group B (*N. albigula* and *N. lepida*), and Group C (*N. floridana* and *N. micropus*). PC1, accounting for 51.3% of outline variation in shape (Table 1), describes the degree of folding along the reentrant on the lingual side of the molar (Fig. 4C). Specimens with lower PC1 values have deeper grooves between the lophs of the M1 and a clear presence of the anterolingual fold. Higher PC1 values correspond to molars with a shallower groove along the lingual side of the tooth and absence of the anterolingual fold. PC2 characterizes 15% of molar shape variation (Table 1) and describes molar width and angle of the lophs in relation to the lingual–buccal plane. Higher PC2 values represent wider molars with the lophs arranged more parallel to one another from anterior to posterior (Fig. 4C). Thinner molars whose lophs have great angling from anterior to posterior have lower PC2 values. PC3 describes variation in the width and spacing of the three lophs, with higher values corresponding to wider lophs and lower PC3 values corresponding to thinner, generally more separated lophs (Fig. 4C).

Despite these clear differences, overall outline analysis could not always assign molars robustly and consistently to the correct species. Indeed, jackknife validation of the CVA on the first three PC scores (representing 76.3% of shape variation; Table 1) identified the correct species only 57% of the time. However, classification of some species was more robust. For example, *N. cinerea* had the highest percent of correct classification (91.1%), followed by *N. lepida* (84.0%). The remaining four species were generally misclassified (Table 3). *Neotoma mexicana* and *N. micropus* molars only were classified to species accurately 16.7% and 10% of the time, respectively. *Neotoma albigula* and *N. floridana* were misclassified in 100% of cases. *Neotoma cinerea* and *N. mexicana* were misclassified most commonly as each other (4.4% and 80%, respectively), and are rarely misclassified with other species (Table 3). In contrast, over half the *N. albigula* (75%) and *N. floridana* (60%) were misclassified as *N. lepida*. *Neotoma micropus* was misclassified as *N. lepida* 45% of the time, and as *N. cinerea* in an additional 40% of cases (Table 3). We found the first CV score to explain 95.5% of the within-group variation in the UM1 of *Neotoma* species, while CV2 and CV3 explained only 3.1% and 1.3%, respectively.

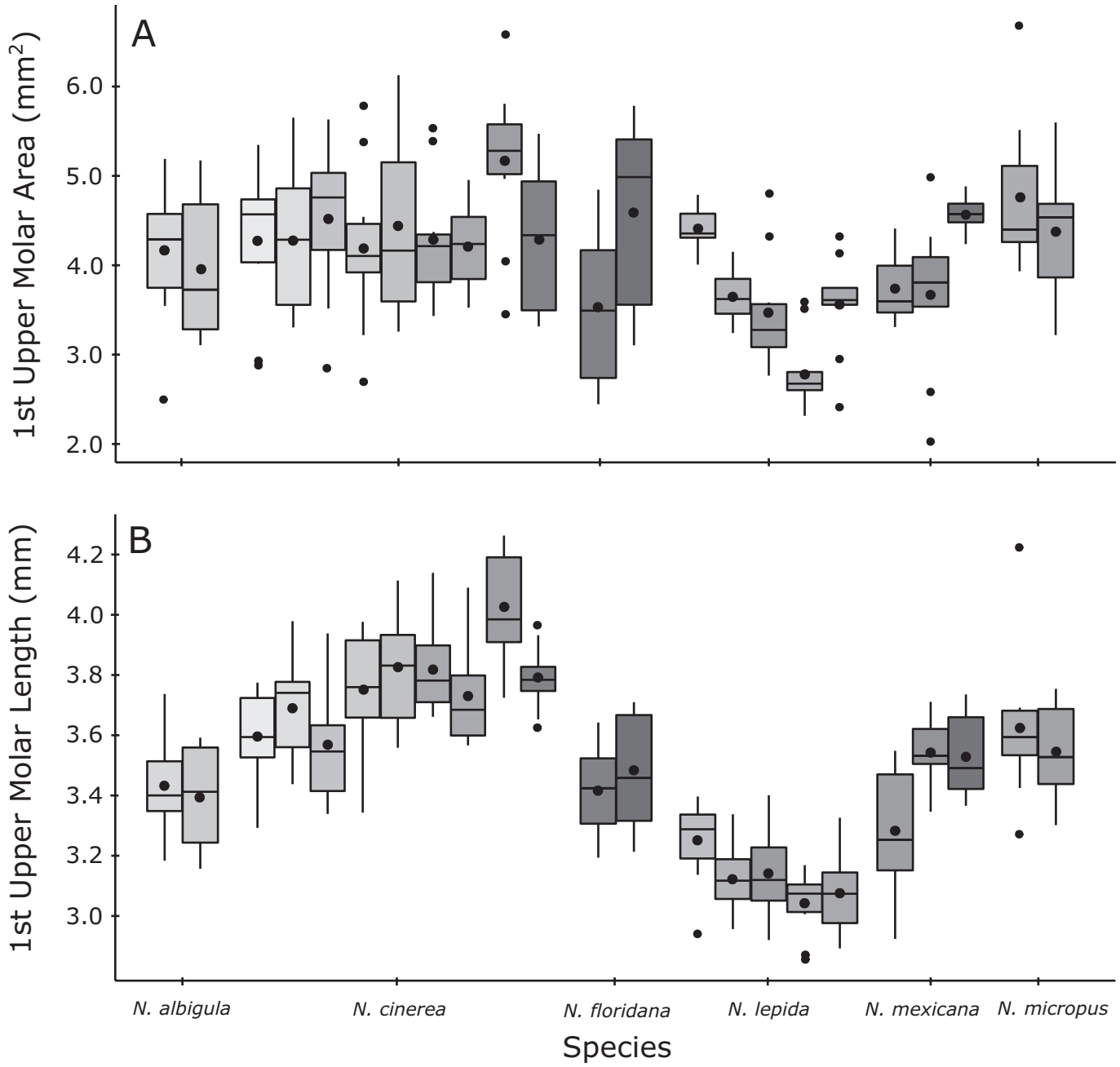

Fig. 3.—Molar length and area across *Neotoma* localities. Distribution of upper first molar (A) area (mm^2) and (B) length (mm) across species of *Neotoma* with localities ranked from lowest to highest latitude (left to right).

Interestingly, jackknife validation testing of how accurately individuals could be classified to locality within species found somewhat different results. Species that were more distinguishable by molar shape across the genus tended to have lower accurate assignments to locality, and vice versa. Every individual of *N. floridana*, for example, was correctly assigned to locality, while *N. cinerea* could only be correctly assigned to locality about 15.6% of the time. Of the remaining species, *N. mexicana* and *N. micropus* individuals were sorted to locality correctly over half the time (63.3% and 60%, respectively), while *N. lepida* and *N. albigula* specimens were placed into their correct localities in 50% and 45% of cases.

Environmental Variables.—We found significant relationships between size and shape and various climate variables and vegetation indices. At the generic level, mean annual precipitation (MAP), mean annual temperature (MAT), and minimum annual temperature (MnAT) gave the lowest ΔAIC model for M1 length (Table 4), with a negative association between temperature and length. Shape variation as characterized by PCs 1–3 were associated significantly with both climate and vegetation, with maximum annual temperature (MxAT) consistently present in all significant models (Table 4) and associated with shallower folding patterns, wider molars, and wider, more closely situated lophs. At the species level, climate was

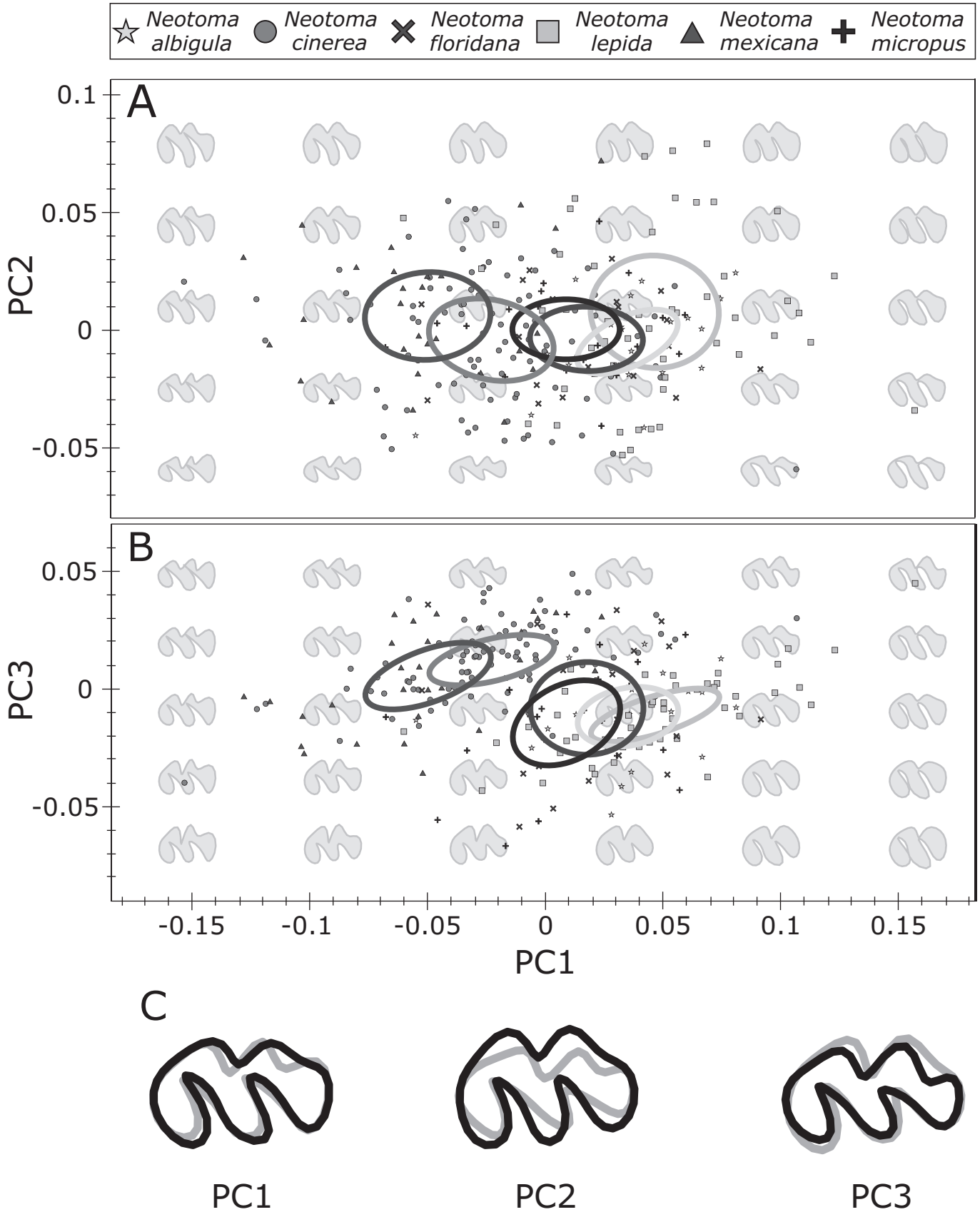

Fig. 4.—Principal components analysis of *Neotoma* molar shape. First three principal components (PCs) plotted against one another for all 230 specimens. Fifty percent confidence ellipses are given for species M1 outline shape. Together, PC1–3 explain 76.3% of variance in shape, with differences being represented by molar shape projections (gray) for (A) PC1 versus PC2, and (B) PC1 versus PC3. (C) +2 *SD* (blue) and −2 *SD* (orange) from mean molar shape show the variance explained by PC1–3.

Table 3.—Percent of *Neotoma* M1 outlines correctly classified to species from canonical variate analysis jackknife cross-validation. Bold values indicate outlines that were correctly assigned to their species over 50% of the time.

		% Classification:					
		Neotoma albigula	*Neotoma cinerea*	*Neotoma floridana*	*Neotoma lepida*	*Neotoma mexicana*	*Neotoma micropus*
Known group:	*N. albigula*	0.0	15.0	0.0	75.0	0.0	10.0
	N. cinerea	0.0	**91.1**	1.1	3.3	4.4	0.0
	N. floridana	0.0	35.0	0.0	60.0	0.0	5.0
	N. lepida	4.0	8.0	0.0	**84.0**	2.0	2.0
	N. mexicana	0.0	80.0	0.0	0.0	16.7	3.3
	N. micropus	5.0	40.0	0.0	45.0	0.0	10.0

associated significantly with molar area in *N. floridana* (MAT), *N. lepida* (MAP, MAT, MnAT), and *N. mexicana* (MAT, MxAT), but no association was found between molar area and vegetation (Table 4). Maximum temperature was significantly and negatively associated with M1 length in *N. mexicana* (Table 4). Molar length in *N. cinerea* was correlated with MAP, MAT, MnAT, and NDVI, and with MxAT, MnAT, and NDVI, in *N. lepida.* Neither the first PC (degree of lingual folding), nor PCs 1–3 together were found to be significantly associated with climate at the species level (Table 4). Mean annual temperature was present in all significant relationships between PC2 or PC3 and climate or vegetation. Minimum annual temperature was important to significant size and shape associations in *N. cinerea*, *N. lepida*, *N. micropus*, while maximum annual temperature was most present in associations across *N. mexicana.* The vegetation index was found to be significantly related to size (M1 length) variation in *N. cinerea*, and *N. lepida*, and shape across all species (PC1 and PC2) and *N. cinerea* (PC3).

Phylogenetic analysis.—Our maximum-likelihood tree topology matched that of Matocq et al. (2007; Fig. 5A). Surprisingly, molar outline shape did not exhibit a significant phylogenetic signal ($K = 0.7075$, P-value > 0.05), suggesting that more closely related *Neotoma* species did not have strong similarities in molar outline. Projection of the phylogenetic tree onto shape space (Fig. 5B) shows a series of overlapping branches and lack of clustering among sister species. Thus, we conclude that overall, phylogeny does not drive the overall patterns in molar shape.

Discussion

We find significant differences in size and shape of *Neotoma* molars. Size was strongly related to temperature and shape was not driven by phylogeny but may instead be related to environment. While elliptical Fourier analysis of molar outline did not provide a general tool for discriminating among all species, it was useful for some comparisons, and moreover suggested a potential link between dental morphology and dietary generalization or specialization both at the species and local level.

Overall, the six species of *Neotoma* examined in this study show varying degrees of differences in the size and shape of the first upper molar. Intraspecifically, species with broad distribution, such as *N. cinerea* and *N. mexicana*, exhibit a strong north to south body size gradient (Cornely and Baker 1986; Smith 1997; Smith and Betancourt 2003; Table 2). When considering all species together, we found mean and minimum annual temperature to be negatively related to M1 length (Table 4). Furthermore, molar length had a negative association with minimum annual temperature in *N. cinerea*, and maximum annual temperature in *N. mexicana*. Because molar length reflects body size, it is likely that molar length's association with temperature is a result of the effect of climate on body size of the genus. *Neotoma cinerea* and *N. mexicana* occupy the northernmost and southernmost latitudes of the genus' range, respectively, such that the species' sensitivity in body size to minimum and maximum annual temperatures makes intuitive sense. As such, *N. cinerea* and *N. mexicana* tend to increase in body size

Table 4.—Multiple regression model results of climate variables and vegetation index to M1 size and shape across species. Models included climate and vegetation variables: mean annual precipitation (MAP), mean annual temperature (MAT), maximum annual temperature (MxAT) and minimum annual temperature (MnAT), normalized difference vegetation index (NDVI) from ClimateWNA (Wang et al. 2016), PRISM (Daly et al. 2008), and NASA EOSDIS Land Processes DAAC (Didan et al. 2015). Significance of models are denoted as follows: ns, not significant, $*P < 0.05$, $**P < 0.01$, and $***P < 0.001$.

Neotoma species	Size variable	Model	Relationship to model variables	ΔAIC	*F*	Adjusted R^2	*d.f.*	Significance
All	PC2	MAP + MAT + MxAT + MnAT + NDVI	*neg., neg., pos., pos., neg.*	0.0	4.92	0.10	5/179	***
All	PC1 + PC2 + PC3	MAP + MxAT	*neg., pos.*	3.3	11.86	0.11	2/182	***
All	PC1	MAP + MxAT + NDVI	*neg., pos., neg.*	3.4	14.35	0.18	3/181	***
All	UM1 Length	MAP + MAT + MnAT	*pos., neg., neg.*	3.8	17.63	0.21	3/181	***
All	UM1 Area	MxAT + NDVI	*pos., neg.*	4.1	2.97	0.02	2/182	ns
All	PC3	MxAT	*neg.*	6.5	18.62	0.09	1/183	***
N. albigula	UM1 Length	MAP + MAT + MxAT	*neg., pos., neg.*	0.0	1.84	0.12	3/16	ns
N. albigula	UM1 Area	MAP + MAT	*neg., pos.*	0.4	1.58	0.06	2/17	ns
N. albigula	PC3	MAP + MxAT	*pos., neg.*	2.0	1.71	0.07	2/17	ns
N. albigula	PC1 + PC2 + PC3	MAT	*pos.*	2.7	2.06	0.05	1/18	ns
N. albigula	PC1	MAT	*pos.*	3.5	2.12	0.06	1/18	ns
N. albigula	PC2	MAT	*pos.*	3.9	0.92	0.00	1/18	ns
N. cinerea	UM1 Length	MAP + MAT + MnAT + NDVI	*pos., pos., neg., pos.*	0.4	3.71	0.14	4/62	**
N. cinerea	PC2	MAT + MxAT + MnAT + NDVI	*neg., pos., pos., neg.*	1.5	1.40	0.01	4/62	ns
N. cinerea	PC3	MAT + NDVI	*pos., pos.*	5.2	4.09	0.09	2/64	*
N. cinerea	PC1	MAT + MnAT	*pos., neg.*	5.6	2.09	0.03	2/64	ns
N. cinerea	PC1 + PC2 + PC3	MxAT	*pos.*	7.5	1.42	0.01	1/65	ns
N. cinerea	UM1 Area	MAP	*pos.*	7.6	0.88	0.00	1/65	ns
N. floridana	PC1	MAT	*neg.*	2.7	1.03	0.00	1/18	ns
N. floridana	PC3	MAT	*pos.*	3.0	50.79	0.72	1/18	***
N. floridana	UM1 Area	MAT	*neg.*	3.7	5.87	0.20	1/18	*
N. floridana	UM1 Length	MAT	*neg.*	3.9	0.79	0.00	1/18	ns
N. floridana	PC1 + PC2 + PC3	MxAT	*neg.*	3.9	3.03	0.10	1/18	ns
N. floridana	PC2	MAP	*pos.*	4.0	0.20	0.00	1/18	ns
N. lepida	PC2	MAT + MxAT + MnAT	*pos., neg., neg.*	2.8	7.53	0.42	3/24	**
N. lepida	UM1 Area	MAP + MAT + MnAT	*neg., pos., neg.*	3.0	8.97	0.47	3/24	***
N. lepida	UM1 Length	MxAT + MnAT + NDVI	*pos., neg., neg.*	4.0	4.05	0.25	3/24	*
N. lepida	PC3	MnAT	*neg.*	6.5	0.19	0.00	1/26	ns
N. lepida	PC1	MxAT	*neg.*	6.6	3.94	0.10	1/26	ns
N. lepida	PC1 + PC2 + PC3	MAP	*neg.*	7.1	1.30	0.01	1/26	ns
N. mexicana	PC3	MAP + MAT + MxAT	*neg., neg., pos.*	0.0	3.77	0.22	3/26	*
N. mexicana	UM1 Area	MAT + MxAT	*pos., neg.*	1.8	8.71	0.35	2/27	**
N. mexicana	PC2	MAT + MxAT	*pos., neg.*	2.0	10.28	0.39	2/27	***
N. mexicana	PC1 + PC2 + PC3	MAT	*neg.*	2.9	0.58	0.00	1/28	ns
N. mexicana	PC1	MxAT	*pos.*	3.2	1.04	0.00	1/28	ns
N. mexicana	UM1 Length	MxAT	*neg.*	3.9	18.19	0.37	1/28	***
N. micropus	PC2	MAT + MxAT + MnAT	*pos., neg., neg.*	2.0	3.25	0.26	3/16	*
N. micropus	PC1	MAT	*neg.*	3.7	0.22	0.00	1/18	ns
N. micropus	PC1 + PC2 + PC3	MAP	*neg.*	4.5	2.35	0.07	1/18	ns
N. micropus	UM1 Area	MAT	*pos.*	4.6	0.69	0.00	1/18	ns
N. micropus	UM1 Length	MxAT	*neg.*	5.0	1.62	0.03	1/18	ns
N. micropus	PC3	MAP	*neg.*	5.5	0.76	0.00	1/18	ns

from southern, warmer localities to northern, colder localities (Table 2; Figs. 1 and 2), conforming to Bergmann's rule (Bergmann 1847; Mayr 1956). *Neotoma lepida* is an exception with southern populations generally larger than northern ones (Verts and Carraway 2002). The temperature gradient across the range of *N. lepida* is east to west, rather than north to south; and indeed, the eastern desert populations are typically smaller than the western mountain populations (Brown and Lee 1969).

Molar shape.—The outline patterns of the *Neotoma* molars in our study may assist classification of *Neotoma* into three morpho-groups, as determined by the degree of folding along the lophs of the M1 and prominence of the anterolingual fold. *Neotoma mexicana* and *N. cinerea* exhibit greater folding of the anterior lophs and a more prominent anterolingual fold (Figs. 2H and 2K), which contrasts the wider lophs with shallower folds and minimal to no development of the anterolingual fold in *N. albigula* and *N. lepida* (Figs. 2G and 2J; 4A and 4B). The mean M1 shape of *N. floridana* and *N. micropus* (Figs. 2I and 2L) tends to exhibit loph and fold characteristics between these two groups. With the exception of *N. micropus*, these results are consistent with those described by Van Devender et al. (1977) and align generally well with Zakrzewski (1993) and Repenning (2004). Those authors found the anterolingual fold to be more prominent within *N. cinerea*, *N. mexicana*, and *N. micropus*, compared to *N. stephensi* (not considered here) and *N. lepida.* However, the results of the jackknife cross-validation (Table 3) suggest that precise classifications to the species level using outline shape alone are not reliable across these six species.

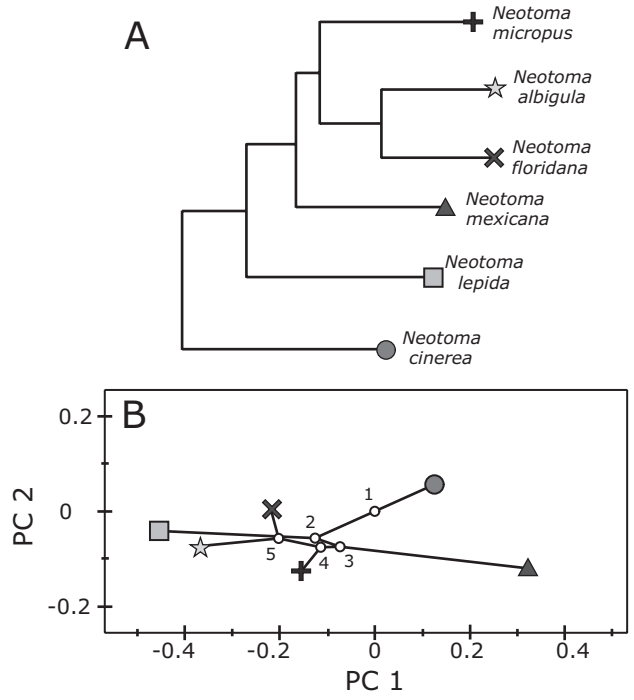

Fig. 5.—*Neotoma* cladogram and phylogeny in shape space. (A) Maximum-likelihood tree topology of *Neotoma* reconstructed from Matocq et al. (2007). (B) Phylogenetic tree of *Neotoma* as projected in morphospace for PC1 and PC2.

We only were able to classify robustly two species based on cross-validation of molar outlines: *N. cinerea* and *N. lepida*. The higher correct classifications of *N. cinerea* and *N. lepida* (Table 3) may be a consequence of a greater number of observations for these two species. While efforts were made to select for specimens within a certain age range, the degree of wear along a molar can cause large variations in the occlusal surfaces of teeth (Harris 1984; Guérécheau et al. 2010; Ledevin et al. 2010; Mitchell 2016). This may play role in species classification. Inclusion of only molars with average wear (wear index of 3) increased classification accuracy somewhat for *N. micropus* (from 10% to 25%) but only slightly for *N. lepida* and *N. mexicana* (Supplementary Data SD5). Interestingly, the greater similarity among species in morphospace does not reflect phylogenetic relationships across the genus (Fig. 5), suggesting ecology may be playing a role in molar shape.

Ecology and phylogeny.—The lack of phylogenetic signal coupled with the grouping of species into three general morpho-groups likely indicates an important relationship with diet, although overall tooth shape likely reflects important selection pressures in the evolutionary history of the genus. Within the six species discussed here, *N. cinerea* and *N. mexicana* consume the least amount of succulent plants (Finley 1958; Cornley and Baker 1986). *Neotoma albigula* and *N. micropus* share similar dietary habits (large quantities of *Opuntia*), while neither *N. lepida* nor *N. floridana* are as dependent on cacti (Vorhies and Taylor 1940; Finley 1958). Species subsisting on softer, more succulent foods (e.g., cacti) have a lower degree of folding along the lophs of their molars. In contrast, larger species such as *N. cinerea* may use a greater amount of tougher or fibrous foods (e.g., juniper oak, seeds, etc.—Finley 1958; Cornley and Baker 1986; Smith 1995, 1997; Wang et al. 2003) and exhibit molars with more prominent folding along the lophs. Because increased folding patterns may provide more efficient grinding across the occlusal surface of the teeth (Kay and Hiiemae 1974; Ungar 2010, Gailer and Kaiser 2014; Gailer et al. 2016), selection pressure may favor greater anterolingual folding (represented by PC1; Figs. 4A–C) in *N. cinerea* and *N. mexicana*, whose populations generally use more varied resources across their ranges.

Interestingly, cross-validation of localities by outline shape showed *N. floridana, N. mexicana*, and *N. micropus*, to be classified correctly 100%, 63.3%, and 60% of the time, respectively, despite their high misclassification rates across species. Furthermore, molar area was significantly different between the two populations of *N. floridana*. The perfect classification of *N. floridana* specimens into proper localities suggests a correlation with different local diets. While *N. floridana* makes use of an array of resources across its range, the species, as with most *Neotoma*, exploits the most abundant resources between localities (Murphy 1952; Rainey 1956; Finley 1958; Wiley 1980). Different selective pressures across populations may favor morphological changes in molar form such that variation between localities is greater. In contrast, *N. cinerea*, which has the most identifiable morphology (Table 4), is only correctly identified about 15.6% of the time at the local level. Inability to classify *N. cinerea* at the local level may reflect a wider range of resources used (Finley 1958) or potentially

an artifact of sample size. This suggests that molar morphology of *N. floridana* closely reflects environmental conditions, while that of *N. cinerea* is more reflective of phylogeny.

The relationship between differences in shape (PC1–3) and climate is not as clear. Species that are more similar in morphospace are not similarly related with temperature and precipitation (Table 4). The first three PC scores are significantly associated with mean annual precipitation and maximum annual temperature across *Neotoma.* PC1 and PC2 are associated with vegetation index, and in this context, the relationship between shape, climate, and vegetation across species suggests individuals experiencing less precipitation, hotter temperatures, or less green vegetation should generally have lophs that are wider with smaller infolding angles between lophs, which tends to align with the desertic *Neotoma* species (*N. albigula* and *N. lepida*).

While outline analysis did not provide a means of consistent classification across all *Neotoma* species, a combined use of size measurements and shape analysis may increase accuracy of molar classifications. For example, use of size information may resolve species within Morpho-Group B because *N. lepida* typically is smaller than *N. albigula.* The variation associated with shared dietary characteristics across the morpho-groups identified suggests that geography and vegetation are both playing a role in driving molar shape evolution, allowing the genus to adapt to a wide array of resources and habitats. Here we used dietary preference derived from the literature to explain morphological patterns. However, in future work, comparing shape variation using detailed resource data, for example, stable isotopes to characterize isotopic niche space, would provide insight into how diet influences dental morphology across the genus. Further insight can then help interpret whether important changes are occurring at regional scales. The abundance of *Neotoma* in the fossil record, and presence of paleomiddens, makes the genus a valuable tool in understanding the Quaternary. Clarifying these ecomorphological traits in *Neotoma* improves our understanding of the Quaternary, and the relationship between the genus and the ecosystem with which they coexisted.

Acknowledgments

We thank Smithsonian National Museum of Natural History and the James F. Bell Museum of Natural History for access to their specimen collections. We thank Jonathan Keller for photographing specimens from the James F. Bell Museum of Natural History. We also thank Dr. Jocie Colella for her assistance with the phylogenetic portion of the molar shape analysis. CPT was supported in part by the National Science Foundation Division of Environmental Biology 1555525 granted to FAS and Seth D. Newsome, and the National Science Foundation Division of Environmental Biology 1744223 granted to S. Kathleen Lyons. WW-J was funded through the 2008 Smithsonian Institution Fellowship Program, helping to make this project possible.

Supplementary Data

Supplementary data are available at *Journal of Mammalogy* online.

Supplementary Data SD1.—Additional methods and results testing for potential biases across specimens assigned different wear indices for both size and shape.

Supplementary Data SD2.—Results of Tukey multiple pairwise comparisons of means for ANOVAs across molar wear indices (2–4) for *Neotoma* specimens included in size and shape analyses.

Supplementary Data SD3.—Number of *Neotoma* specimens for each wear index by species.

Supplementary Data SD4.—Results of Tukey multiple comparisons of means for ANOVA of molars with a medium wear index (3). Significant *P*-values (*P*) are in bold.

Supplementary Data SD5.—Percent of *Neotoma* M1 outlines correctly classified to species from canonical variate analysis jackknife cross-validation from subset of specimens with wear indices of 3.

Literature Cited

Adams, D. C. 1999. Methods for shape analysis of landmark data from articulated structures. Evolutionary Ecology Research 1:959–970.

Adams, D. C., F. J. Rohlf, and D. E. Slice. 2004. Geometric morphometrics: ten years of progress following the 'revolution.' Italian Journal of Zoology 71:5–16.

Adams, D. C., M. L. Collyer, and A. Kaliontzopoulou. 2018. Geomorph: software for geometric morphometric analyses. R package version 3.0.6. https://cran.r-project.org/package=geomorph. Accessed 18 January 2019.

Adebowale, A., A. Nicholas, J. Lamb, and Y. Naidoo. 2012. Elliptic Fourier analysis of leaf shape in southern African *Strychnos* section *Densiflorae* (Loganiaceae). Botanical Journal of the Linnean Society 170:542–553.

Bergmann, C. 1847. Über die Verhältnisse der Wärmeökonomie der Thiere zu ihrer Größe. Gottinger Studien 1:595–708.

Betancourt, J. L., T. R. Van Devender, and P. S. Martin (eds.). 1990. Packrat middens: the last 40,000 years of biotic change. University of Arizona Press. Tucson.

Bonhomme, V., S. Picq, and J. Claude. 2012. Momocs package. http://cran.r-project.org/web/packages/Momocs/index.html. Accessed 2 May 2018.

Bonhomme, V., S. Picq, C. Gaucherel, and J. Claude. 2014. Momocs: outline analysis using R. Journal of Statistical Software 56:1–24.

Bonhomme, V., S. Prasad, and C. Gaucherel. 2013. Interspecific variability of pollen morphology as revealed by elliptic Fourier analysis. Plant Systematics and Evolution 299:811–816.

Bookstein, F. L. 1997. Morphometric tools for landmark data: geometry and biology. Cambridge University Press. Cambridge, United Kingdom.

Braun, J. K., and M. A. Mares. 1989. *Neotoma micropus*. Mammalian Species 330:1–9.

Brown, J. H. 1968. Adaptation to environmental temperature in two species of woodrats, *Neotoma cinerea* and *N. albigula*. Miscellaneous Publications, Museum of Zoology, University of Michigan 135:1–48.

Brown, J. H., and A. K. Lee. 1969. Bergmann's rule and climatic adaptation in woodrats (*Neotoma*). Evolution 23:329–338.

Cameron, G. N., and D. G. Rainey. 1972. Habitat utilization by *Neotoma lepida* in the Mohave desert. Journal of Mammalogy 53:251–266.

Carey, A. B. 1991. The biology of arboreal rodents in Douglas-fir forests. General Technical Report PNW-GTR-276. US Department of Agriculture, Forest Service, Pacific Northwest Research Station, Portland, Oregon.

Carrasco, M. A. 2000. Species discrimination and morphological relationships of kangaroo rats (*Dipodomys*) based on their dentition. Journal of Mammalogy 81:107–122.

Carraway, L. N., and B. J. Verts. 1991. *Neotoma fuscipes*. Mammalian Species 386:1–10.

Claude, J. 2008. Morphometrics with R. Springer Science & Business Media. New York.

Cornely, J. E., and R. J. Baker. 1986. *Neotoma mexicana*. Mammalian Species 262:1–7.

Dalquest, W. W., E. Roth, and F. Judd. 1969. The mammal fauna of Schulze Cave, Edwards County, Texas. Bulletin of the Florida State Museum 13:205–276.

Daly, C., R. P. Neilson, and D. L. Phillips. 1994. A statistical topographic model for mapping climatological precipitation over mountainous terrain. Journal of Applied Meteorology 33:140–158.

Daly, C., et al. 2008. Physiographically sensitive mapping of climatological temperature and precipitation across the conterminous United States. International Journal of Climatology 28:2031.

Dial, K. P. 1988. Three sympatric species of *Neotoma*: dietary specialization and coexistence. Oecologia 76:531–537.

Didan, K., A. Munon, R. Solano, and A. Huerte. 2015. MODIS Vegetation Index User's Guide (MODIS13 Series). Vegetation Index Phenology Lab, The University of Arizona. 1–35.

Edgar, R. C. 2004. MUSCLE: multiple sequence alignment with high accuracy and high throughput. Nucleic Acids Research 32:1792–1797.

Evans, A. R., and G. D. Sanson. 2003. The tooth of perfection: functional and spatial constraints on mammalian tooth shape. Biological Journal of the Linnean Society 78:173–191.

Evans, A. R., G. P. Wilson, M. Fortelius, and J. Jernvall. 2007. High-level similarity of dentitions in carnivorans and rodents. Nature 445:78–81.

Finley, R. B. 1958. The wood rats of Colorado: distribution and ecology. University of Kansas. Lawrence.

Fortelius, M. 1985. Ungulate cheek teeth: developmental, functional, and evolutionary interrelations. Acta Zoologica Fennica 180:1–76.

Friess, M., and M. Baylac. 2003. Exploring artifical cranial deforamation using ellipitical fourier analysis of Procrustes aligned outlines. American Journal of Physical Anthropology 122:11–22.

Gailer, J. P., I. Calandra, E. Schulz-Kornas, and T. M. Kaiser. 2016. Morphology is not destiny: discrepancy between form, function and dietary adaptation in bovid cheek teeth. Journal of Mammalian Evolution 23:369–383.

Gailer, J. P., and T. M. Kaiser. 2014. Common solutions to resolve different dietary challenges in the ruminant dentition: the functionality of bovid postcanine teeth as a masticatory unit. Journal of Morphology 275:328–341.

Gómez Cano, A. R., M. Hernández Fernández, and M. Á. Alvarez-Sierra. 2013. Dietary ecology of Murinae (Muridae, Rodentia): a geometric morphometric approach. PLoS ONE 8:e79080.

Guérécheau A., et al. 2010. Seasonal variation in molar outline of bank voles: an effect of wear? Mammalian Biology 75:311–319.

Hall, E. R. 1981. The mammals of North America. 2nd ed. Wiley & Sons. New York.

Harris, A. H. 1984. *Neotoma* in the late Pleistocene of New Mexico and Chihuahua. Special Publications, Carnegie Museum of Natural History 8:164–178.

Hickling, G. J. 1987. Seasonal reproduction and group dynamics of bushy-tailed woodrats, *Neotoma cinerea*. Ph.D. dissertation, The University of Western Ontario. London, Ontario, Canada.

Hillson, S. 2005. Teeth. Cambridge University Press. New York.

IUCN. 2018. The IUCN red list of threatened species. Ver. 2018.2. http://www.iucnredlist.org. Accessed 15 March 2018.

Janis, C. M. 1995. Correlation between craniofacial morphology and feeding behavior in ungulates: reciprocal illumination between living and fossil taxa. Pp. 76–98 in Functional morphology in vertebrate paleontology (J. J. Thomason, ed.). Cambridge University Press. Cambridge, United Kingdom.

Janis, C. M., and M. Fortelius. 1988. On the means whereby mammals acieve increased functional durability of their dentitions, with special reference to limiting factors. Biological Reviews 63:197–230.

Jardine, P. E., C. M. Janis, S. Sahney, and M. J. Benton. 2012. Grit not grass: concordant patterns of early origin of hypsodonty in Great Plains ungulates and Glires. Palaeogeography, Palaeoclimatology, Palaeoecology 365–366:1–10.

Jones, C., and N. J. Hildreth. 1989. *Neotoma stephensi*. Mammalian Species 328:1–3.

Kay, R. F., and K. M. Hiiemae. 1974. Jaw movement and tooth use in recent and fossil primates. American Journal of Physical Anthropology 40:227–256.

Kuhl, F. P., and C. R. Giardina. 1982. Elliptic Fourier features of a closed contour. Computer Graphics and Image Processing 18:236–258.

Ledevin, R., J. P. Quéré, and S. Renaud. 2010. Morphometrics as an insight into processes beyond tooth shape variation in a bank vole population. PLoS ONE 5:e15470.

Macêdo, R. H., and M. A. Mares. 1988. *Neotoma albigula*. Mammalian Species 310:1–7.

Matocq, M. D., Q. R. Shurtliff, and C. R. Feldman. 2007. Phylogenetics of the woodrat genus *Neotoma* (Rodentia: Muridae): implications for the evolution of phenotypic variation in male external genitalia. Molecular Phylogenetics and Evolution 42:637–652.

Mayr, E. 1956. Geographical character gradients and climatic adaptation. Evolution 10:105–108.

Meiri, S., T. Dayan, and D. Simberloff. 2005. Variability and correlations in carnivore crania and dentition. Functional Ecology 19:337–343.

Meserve, P. L. 1974. Ecological relationships of two sympatric woodrats in a California coastal sage scrub community. Journal of Mammalogy 55:442–447.

Mitchell J. 2016. Application of micro-CT and elliptic Fourier analysis on molar outline shape for group discrimination of notoungulates. Ph.D. dissertation, University of California, Santa Barbara. Santa Barbara.

Murphy, M. F. 1952. Ecology and helminths of the Osage wood rat, *Neotoma floridana osagensis*, including the description of *Longistriata neotoma* n. sp. (Trichostrongylidae). American Midland Naturalist 48:204–218.

Olsen, R. W. 1976. Water: a limiting factor for a population of wood rats. The Southwestern Naturalist 21:391–398.

Orr, T. J., S. D. Newsome, and B. O. Wolf. 2015. Cacti supply limited nutrients to a desert rodent community. Oecologia 178:1045–1062.

Patton, J. L., D. G. Huckaby, and S. T. Álvarez-Castaneda. 2007. The evolutionary history and a systematic revision of woodrats of the *Neotoma lepida* group. University of California Publications in Zoology, University of California Press. Berkeley.

R Development Core Team. 2016. R: a language and environment for statistical computing. R Foundation for Statistical Computing. Vienna, Austria. www.R-project.org/. Accessed 15 July 2016.

Rainey, D. G. 1956. Eastern woodrat, *Neotoma floridana*: life history and ecology. University of Kansas Publications, Museum of Natural History 8:535–646.

Rasband, W. S. 1997–2018. ImageJ. U.S. National Institutes of Health. Bethesda, Maryland. https://imagej.nih.gov/ij/. Accessed 15 July 2016.

Renaud, S., J. Michaux, J. J. Jaeger, and J. C. Auffray. 1996. Fourier analysis applied to *Stephanomys* (Rodentia, Muridae) molars: nonprogressive evolutionary pattern in a gradual lineage. Paleobiology 22:255–265.

Renaud, S., and V. Millien. 2001. Intra-and interspecific morphological variation in the field mouse species *Apodemus argenteus* and *A. speciosus* in the Japanese archipelago: the role of insular isolation and biogeographic gradients. Biological Journal of the Linnean Society 74:557–569.

Repenning, C. A. 2004. Fossil wood rats of Porcupine Cave: tectonic or climatic controls. Pp. 193–206 in Biodiversity response to climate change in the middle Pleistocene: the Porcupine cave fauna from Colorado (A. D. Barnosky, ed.). University of California Press. Berkeley.

Rodrigues, H. G., et al. 2013. Roles of dental development and adaptation in rodent evolution. Nature Communications 4:2504.

Rohlf, F. J. 1990. Morphometrics. Annual Review of Ecology and Systematics 21:299–316.

Rohlf, F. J., and D. Slice. 1990. Extensions of the Procrustes method for the optimal superimposition of landmarks. Systematic Biology 39:40–59.

RStudio Team. 2016. RStudio: integrated development for R. RStudio Inc. Boston, Massachusetts.

Samuels, J. X. 2009. Cranial morphology and dietary habits of rodents. Zoological Journal of the Linnean Society 156:864–888.

Samuels, J. X., and S. S. B. Hopkins. 2017. The impacts of Cenozoic climate and habitat changes on small mammal diversity of North America. Global and Planetary Change 149:36–52.

Schlager, S. 2017. Morpho and Rvcg - shape analysis in R. Pp. 217–256 in Statistical shape and deformation analysis (G. Zheng, S. Li, and G. Szekely, eds.). Academic Press. London, United Kingdom.

Schmidly, D. J., and R. D. Bradley. 2016. The mammals of Texas. University of Texas Press. Austin.

Schmidt-Kittler, N. 2002. Feeding specializations in rodents. Senckenbergiana Lethaea 82:141–152.

Smith, F. A. 1995. Scaling of digestive efficiency with body mass in *Neotoma*. Functional Ecology 9:299–305.

Smith, F. A. 1997. *Neotoma cinerea*. Mammalian Species 564:1–8.

Smith, F. A., and J. L. Betancourt. 2003. The effect of Holocene temperature fluctuations on the evolution and ecology of *Neotoma* (woodrats) in Idaho and northwestern Utah. Quaternary Research 59:160–171.

Smith, F. A. and J. L. Betancourt. 2006. Predicting woodrat (*Neotoma*) responses to anthropogenic warming from studies of the palaeomidden record. Journal of Biogeography 33:2061–2076.

Smith, F. A., J. L. Betancourt, and J. H. Brown. 1995. Evolution of body size in the woodrat over 25000 years of climate change. Science 270:2012–2014.

Smith, F. A., et al. 2009. A tale of two species: extirpation and range expansion during the late quaternary in an extreme environment. Global and Planetary Change 65:122–133.

Stamatakis, A. 2014. RAxML version 8: a tool for phylogenetic analysis and post-analysis of large phylogenies. Bioinformatics 30:1312–1313.

Strait, S. G. 1993a. Differences in occlusal morphology and molar size in frugivores and faunivores. Journal of Human Evolution 25:471–484.

Strait, S. G. 1993b. Molar morphology and food texture among small-bodied insectivorous mammals. Journal of Mammalogy 74:391–402.

Thomason, J. (ed.). 1997. Functional morphology in vertebrate paleontology. Cambridge University Press. New York, NY, USA.

Travis, J. 1994. Evaluating the adaptive role of morphological plasticity. Pp. 99–122 in Ecological morphology: integrative organismal biology (P. C. Wainwright and S. M. Reilly, eds.). The University of Chicago Press. Chicago, Illinois.

Ungar, P. S. 2010. Mammal teeth: origin, evolution, and diversity. Johns Hopkins University Press. Baltimore, Maryland, USA.

Ungar, P., and M. Williamson. 2000. Exploring the effects of tooth wear on functional morphology: a preliminary study using dental topographic analysis. Palaeontologia Electronica 3:1–18.

Van Devender, T. R., A. M. I. Phillips, and J. I. Mead. 1977. Late Pleistocene reptiles and small mammals from the lower Grand Canyon of Arizona. The Southwestern Naturalist 22:49–66.

Van Valkenburgh, B. 1989. Carnivore dental adaptations and diet: a study of trophic diversity within guilds. Pp. 410–436 in Carnivore behavior, ecology and evolution (J. L. Gittleman, ed.). Springer. Boston, Massachusetts.

Van Valkenburgh, B. 1994. Ecomorphological analysis of fossil vertebrates and their paleocommunities. Pp. 140–166 in Ecological morphology: integrative organismal biology (P. C. Wainwright and S. M. Reilly, eds.). University of Chicago Press. Chicago, Illinois.

Verts, B. J., and L. N. Carraway. 2002. *Neotoma lepida*. Mammalian Species 699:1–12.

Vorhies, C. T., and W. P. Taylor. 1940. Life history and ecology of the white-throated wood rat, *Neotoma albigula* Hartley, in relation to grazing in Arizona. College of Agriculture, University of Arizona, College of Agriculture. Tucson.

Wang, T., A. Hamann, D. L. Spittlehouse, and T. Q. Murdock. 2016. ClimateWNA—high-resolution spatial climate data for western North America. Journal of Applied Meteorology and Climatology 51:16–29.

Wang, D. H., Y. X. Pei, J. C. Yang, and Z. W. Wang. 2003. Digestive tract morphology and food habits in six species of rodents. Folia Zoologica-Praha 52:51–56.

Wiley, R. W. 1980. *Neotoma floridana*. Mammalian Species 139:1–7.

Williams, S. H., and R. F. Kay. 2001. A comparative test of adaptive explanations for hypsodonty in ungulates and rodents. Journal of Mammalian Evolution 8:207–229.

Zakrzewski, R. J. 1993. Morphological change in woodrat (Rodentia: Cricetidae) molars. Pp. 392–409 in Morphological change in Quaternary mammals of North America (R. A. Martin and A. D. Barnosky, eds.). Cambridge University Press. Cambridge, United Kingdom.

Zelditch, M., D. L. Swiderski, and H. D. Sheets. 2012. Geometric morphometrics for biologists: a primer. 2nd ed. Academic Press. Amsterdam, The Netherlands.

Submitted 10 December 2019. Accepted 29 July 2020.

Associate Editor was John Scheibe.

Appendix I Locality and accession information for Neotoma specimens used in analysis. Museum IDs correspond to the Smithsonian National Museum of Natural History (USNM) in Washington, D.C., the Bell Museum of Natural History (MMNH) at the University of Minnesota (St. Paul, Minnesota).

Species	Locality name	State (country)	Latitude	Longitude	*N*	Museum IDs
Neotoma albigula	Grants	New Mexico (United States)	35.15	−107.85	10	USNM: 137714, 137716, 137718, 137719, 137739, 138159, 138160, 138161, 138164, 138167
	Pima	Arizona (United States)	31.86	−110.71	10	USNM: 251307, 251312, 251313, 251314, 251315, 251318, 251319, 251320, 251321, 251326
Neotoma cinerea	Bennett City	British Columbia (Canada)	59.84	−134.99	10	USNM: 128218, 128588, 128589, 128590, 130204, 130205, 130206, 130207, 130208, 130209
	Jaspar House	Alberta (Canada)	52.95	−118.14	10	USNM: 75899, 75900, 75901, 75902, 75905, 75906, 75907, 75910, 75915, 75917
	Spokane	Washington (United States)	47.26	−117.71	10	USNM: 24188, 24189, 24190, 24191, 74775, 74778, 74779, 74780, 230075, 230462
	Klickitat	Washington (United States)	45.70	−120.76	10	USNM: 57139, 89738, 89742, 89743, 226192, 226193, 226194, 226196, 226198, 230460
	Big Horn	Montana (United States)	45.60	−107.46	10	USNM: 214708, 214709, 214710, 214711, 214723, 214724, 214725, 214726, 214727, 214728
	Harney	Oregon (United States)	42.98	−119.00	10	USNM: 79349, 79375, 79382, 80177, 80179, 80180, 205246, 216030, 216035, 222339
	Sweetwater	Wyoming (United States)	42.08	−110.04	10	USNM: 88297, 176909, 177489, 179306, 179307, 179308, 179477, 179478, 179479, 179480
	Bear Lake	Utah and Idaho (United States)	41.67	−111.79	10	USNM: 55181, 55381, 55382, 158533, 167507, 190335, 190336, 263987, 264308, 264309
	Donner	California (United States)	39.21	−120.01	10	USNM: 55547, 55780, 55783, 88327, 88328, 88329, 88330, 88331, 88332, 100661
Neotoma floridana	Wakarusa	Kansas (United States)	38.89	−95.31	10	MMNH: 12621, 12622, 12623, 12627, 12628, 12629, 12630, 12631, 12632, 12633
	Osage	Oklahoma (United States)	36.96	−96.57	10	MMNH: 10254, 11399, 11400, 11401, 11403, 11404, 12642, 12643, 12644, 12646
Neotoma lepida	Secret Valley	Nevada (United States)	40.72	−119.48	10	USNM: 67896, 67897, 78280, 78283, 78284, 78285, 78286, 78288, 94255, 94258
	Coso	California (United States)	36.18	−117.65	10	USNM: 28039, 28042, 28044, 28045, 28049, 28292, 28293, 28302, 28303, 28305
	Lees Ferry	Arizona (United States)	36.06	−112.13	10	USNM: 161167, 161169, 161171, 161173, 161175, 215542, 215543, 215544, 215638, 243126
	Panamint Valley	California (United States)	35.33	−116.10	10	USNM: 25343, 25344, 25345, 25346, 25347, 25348, 25349, 25350, 25351, 25356
	Oro Grande	California (United States)	34.60	−117.34	10	USNM: 136141, 136143, 136145, 136146, 136149, 136150, 136153, 136154, 136155, 136157
Neotoma mexicana	Loveland	Colorado (United States)	40.41	−105.10	10	USNM: 87674, 87677, 87678, 87679, 87680, 87681, 87682, 87921, 87922, 87923
	Manzano Mountains	New Mexico (United States)	34.71	−106.41	10	USNM: 131665, 131672, 131677, 131855, 131860, 131861, 131863, 131866, 131872, 131873
	Omiltemi	Guerrero (Mexico)	17.54	−99.52	10	USNM: 126892, 126920, 126923, 127498, 127499, 340638, 340641, 340642, 340643, 340645
Neotoma micropus	Fort Supply	Oklahoma (United States)	36.57	−99.57	10	USNM: 273225, 273227, 273232, 273322, 273323, 273325, 273326, 273327, 273328, 273699
	Major	Oklahoma (v)	36.17	−98.92	10	MMNH: 12704, 12705, 12706, 12709, 12710, 12711, 12712, 12714, 12717, 12718